Food Chemistry: X 26 (2025) 102303

Contents lists available at ScienceDirect

Food Chemistry: X

journal homepage: www.sciencedirect.com/journal/food-chemistry-x

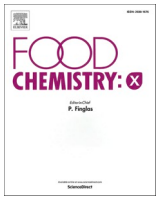

Preparation and application of chitosan/nano-TiO_2/daisy essential oil composite films in the preservation of *Actinidia arguta*

Yue Wang [a], Yu Zhang [a], Yaomei Ma [a], Jiaxin Liu [b], Ruinting Zhang [c], Jun Zhao [a,d,*]

[a] College of Food Science and Engineering, Changchun University, No.6543 Satellite Road, 130022 Changchun, China
[b] Jilin Province Product Quality Supervision and Inspection Institute, Changchun 130103, China
[c] Agriculture College, Yanbian University, Yanbian 133002, China
[d] Key Laboratory of Intelligent Rehabilitation and Barrier-free for the Disabled Ministry of Education, Ministry of Education, Changchun University, Changchun 130022, China

ARTICLE INFO

Keywords:
Chitosan
Nano
Actinidia arguta

ABSTRACT

Chitosan, a natural polysaccharide, is widely recognized for its biocompatibility, biodegradability, and film-forming properties, making it an ideal candidate for food preservation applications. This study focuses on the development of chitosan-based nanocomposite films incorporating nano-TiO_2 and Daisy Essential Oil for the preservation of *Actinidia arguta*. The composite films were synthesized and characterized using FT-IR, XRD, SEM, TGA, UV–Visible spectroscopy, and contact angle measurements to evaluate their structural, thermal, and physical properties. The films exhibited enhanced mechanical strength, antimicrobial activity, and antioxidant capacity. Application of these films on *Actinidia arguta* demonstrated significant improvements in weight loss, hardness, decay rate, total microbial count, respiration rate, soluble solids content, vitamin C, titratable acidity, and enzyme activities during storage. The results indicate that chitosan/nano-TiO_2/DEO composite films effectively extend the shelf life and maintain the quality of *Actinidia arguta*, providing a promising approach for natural and sustainable food preservation.

1. Introduction

Current food preservation methods, particularly for fruits and vegetables, include refrigeration, freezing technologies, modified atmosphere packaging (MAP), edible films, coatings, and active packaging techniques(Liu Wang et al., 2024). Although refrigeration and freezing effectively slow microbial growth by reducing temperature, they require substantial energy consumption and may alter the texture and flavor of fruits and vegetables(Cao et al., 2023; Park et al., 2021). MAP regulates gas ratios within the storage environment, suppressing respiration and microbial growth, but it necessitates specialized storage chambers, resulting in high operational costs.

In comparison, edible films, coatings, and active packaging technologies have attracted attention for their ability to provide a protective layer on the surface of fruits and vegetables, blocking oxygen, moisture, and microorganisms to delay oxidation and spoilage(Wang Yuan, Liu, Li, & Wu, 2024). Chitosan (CS), with its wide availability, low cost, excellent film-forming ability, biocompatibility, and non-toxicity, has become a preferred natural preservative for food applications. CS is extensively used in edible films, coatings, and active packaging technologies, ensuring safety, preserving the natural flavor and nutrients of foods, and promoting sustainability(Heras, Huang, Chang, & Lu, 2024). However, pure chitosan films exhibit some limitations, such as low tensile strength, limited antimicrobial activity, and weak antioxidant properties. To overcome these limitations, researchers have developed CS-based composite films by incorporating other bioactive substances. Current research has primarily followed well-established methods for preparing films and characterizing their properties(Li Wang, Ma, Zheng, Liu, & Liu, 2024; Xue, Wu, Feng, & Kou, 2023). However, there remains a lack of systematic investigation into the preservation effects of different film formulations under both light and dark conditions, especially when combining various additives such as chitosan, essential oils, and nanoparticles. While the characterization of film properties has been extensively studied, comparative research on the preservation performance of films with different combinations of additives, especially under varied environmental conditions, is limited. Furthermore, while numerous studies have addressed the individual contributions of each component, systematic studies that compare the effects of various

* Corresponding author at: College of Food Science and Technology Changchun University, No.8326 Weixing Street, Changchun, Jilin 130022, China.
E-mail address: zhaoJ70@ccu.edu.cn (J. Zhao).

https://doi.org/10.1016/j.fochx.2025.102303
Received 12 January 2025; Received in revised form 5 February 2025; Accepted 18 February 2025
Available online 19 February 2025

additive combinations on the preservation of fresh produce, especially under light exposure versus dark storage, are still sparse. Nano-TiO_2 offers advantages such as high chemical stability, small particle size, high surface activity, non-toxicity, effective antibacterial performance, and good photosensitivity. Additionally, Daisy Essential Oil (DEO) possesses excellent antioxidant properties, and non-toxicity, and can enhance the mechanical performance of pure chitosan films. DEO is purchased from a commercial supplier(Yuanye Biotechnology Co.), with a low addition amount (0.5 %), low cost, suitable for industrial production, and can be applied in food preservation. This study aims to address these gaps by systematically exploring the preservation effects of chitosan-based composite films incorporating nano-TiO_2 and DEO under both light and dark storage conditions. By evaluating the physical, mechanical, and antimicrobial properties of these films, we aim to better understand the role of different additive combinations in prolonging the shelf life and maintaining the quality of food.

Actinidia arguta is a small fruit， rich in many vitamins and minerals， especially vitamin C is much higher than other fruits (Macedo, Costa, & Rodrigues, 2023). Its fruits are small and numerous, and each plant produces a large number of fruits(Pinto, Delerue-Matos, & Rodrigues, 2020)， which has high economic benefits and market potential. The fruit flesh is soft and juicy and has a variety of health benefits, such as promoting digestion, enhancing immunity, and lowering blood lipids and blood pressure. However, the soft date kiwi fruit has thin and fragile skin, high water content, susceptibility to microbial infections after picking, and a short storage period(Xiong, Zhou, Jiang, Yang, & Hu, 2024)， which are problems that have not yet been solved. This research evaluates the preservation efficacy of chitosan/nano-TiO_2/DEO (CSTD) composite films on *Actinidia arguta* under both light and dark conditions, aiming to extend its shelf life and enhance its commercial value. The findings provide theoretical insights into the development of CS-based composite preservation materials.

2. Materials and methods

2.1. Materials and methods

Chitosan (CS) (degree of deacetylation 80–95 %): Purchased from Sinopharm Chemical Reagent Co., Ltd.; Nano-TiO_2 (5–10 nm): Sourced from Macklin Biochemical Co., Ltd., Shanghai; Daisy Essential Oil (DEO) (AR grade): Supplied by Yuanye Biotechnology Co. (CAS No.S27260), Citric Acid (AR grade): Beijing Chemical Works; Glycerol (AR grade): Tianjin Damao Chemical Reagent Factory; Tween 80 (AR grade): Macklin Biochemical Co., Ltd., Shanghai.

2.2. Equipment and instruments

Electronic Balance (AL204): Huazhi Fujian Electronic Technology Co., Ltd.; Thermostatic Magnetic Stirrer (DF-101S): Gongyi Yuhua Instrument Co., Ltd.; Universal Testing Machine (QJ210-50 N): Huaye Scientific Instruments, Jilin; High-Shear Emulsifier (FA30D): Shanghai Fluco Technology Development Co., Ltd.; Oven (GFL-230): Tianjin Laitai Scientific Instrument Co, Ltd.; Digital Thickness Gauge (H346): Guangzhou Xinhe Grating Digital Co, Ltd.; UV–Vis Spectrophotometer (T-6vm): Nanjing Feile Instrument Co, Ltd.; FT-IR Spectrometer (NICOLET iS5): Huaye Scientific Instruments, Jilin; X-ray Diffractometer (UV-2700): Suzhou Langsheng Scientific Instruments Co, Ltd.; Scanning Electron Microscope (SEM) (XL-30 ESEM FEG): Beijing OPTO-TECH Co, Ltd.; Contact Angle Meter (SL200KS): Shanghai Langgan Laboratory Equipment Co, Ltd.; Constant temperature and humidity box(150*RH*) Jilin Channel Science and Education Instrument Co, Ltd.; Thermogravimetric Analyzer (TGA) (Mettler TGA2): PerkinElmer, USA.

2.3. Preparation of composite films

As shown in Fig. 1 the composite film was prepared using the casting

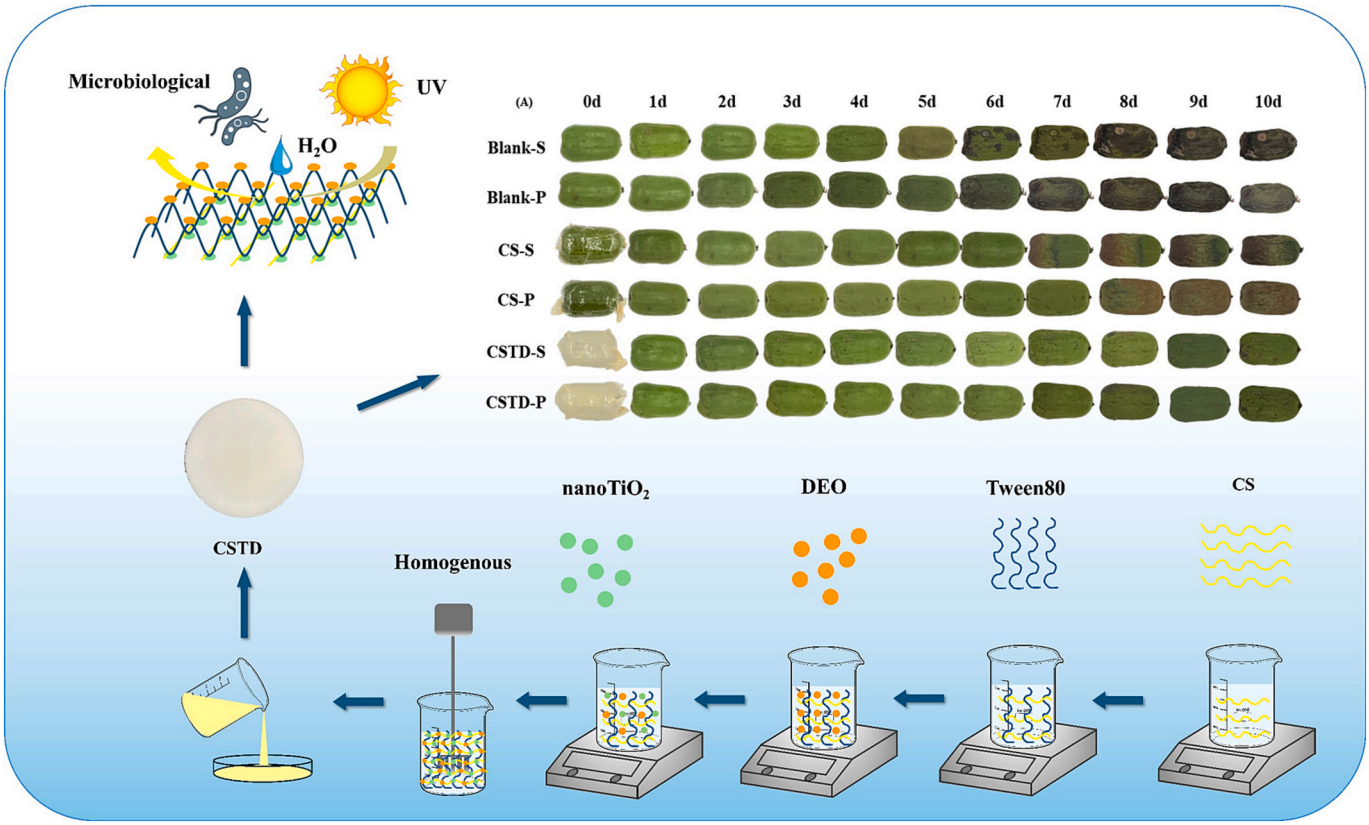

Fig. 1. CSTD research process.

method (Sharma & Dhamodharan, 2024). First, 2 % chitosan was dissolved in a 4 % citric acid solution under stirring at room temperature until the chitosan was fully dissolved, which took approximately 2–3 h. Once the chitosan was completely dissolved, the following components were added sequentially to the solution: Glycerol (0.5 %), Tween 80 (0.25 %), DEO (0.5 %), and nano-TiO_2 (0.4 %). After each addition, the solution was gently stirred to ensure thorough mixing. The resulting mixture was then homogenized using a high-shear emulsifier at 25,000 rpm for 2 min to achieve a uniform dispersion of the DEO and nano-TiO_2 throughout the chitosan matrix. The resulting solution (30 g) was poured into a 9-mm diameter Petri dish and dried in an oven at 50 °C for 5 h. The films were then carefully removed and stored for further testing. Wherein, CS is a single CS film, CSD is a CS/DEO composite film, CST is a CS/nano-TiO_2 composite film, and CSTD is a CS/nano-TiO_2/DEO composite film.

2.4. Measurement of physical and chemical properties

2.4.1. FT-IR analysis

FT-IR spectra were recorded to identify functional groups. The films were dried thoroughly, mixed with KBr at a 1:180 ratio, and pressed into transparent pellets. Each sample was scanned 30 times within the 500–4000 cm^{-1} range.

2.4.2. XRD analysis

X-ray diffraction was performed using a BRUKER XRD system to determine the crystalline condition of the samples. Scans were performed between 10° and 70° at a rate of 5°/min under Cu-Kα radiation (40 kV, 40 mA).

2.4.3. SEM analysis

The surface morphology of the films was observed using SEM. Samples were mounted on adhesive-coated stubs, sputter-coated with gold, and examined under magnifications of 200, 5000, and 20,000×.

2.4.4. TGA analysis

Film samples (4–6 mg) were sealed in platinum pans and heated from 30 °C to 600 °C at a rate of 10 °C/min under a nitrogen atmosphere. Changes in mass are recorded continuously as a function of temperature.

2.4.5. UV–visible analysis

Determination was carried out using a UV spectrophotometer, the sample was cut into 1 cm × 1 cm strips and placed in the sample chamber with a wavelength scanning range of 200-430 nm.

2.4.6. Measurement of mechanical and antimicrobial properties

Determine the tensile strength (TS) and elongation at break (EB) of the composite film using a universal measuring instrument, cut the film into strips of 10 mm × 5 mm, fixed in the measuring instrument, and then measured at a speed of 20 mm/min. Each film sample was measured three times, and the average value was calculated using eqs. (1) and (2) as follows.

$$TS = F/(\mathrm{b} \times \mathrm{d}) \tag{1}$$

$$EB = \Delta L/L \times 100\% \tag{2}$$

where: TS-Tensile strength, MPa; F-Fracture strength, N; b-Sample width, mm; d-Film thickness, mm; EB-Elongation, %; ΔL-Total deformation, cm; L-original scale length, cm.

The use of a digital film thickness gauge, in the composite cling film on the randomly selected 6 points to measure the thickness of the film, each group of test specimens to do 3 parallel tests, the average of which is recorded as the thickness of the film.

Anhydrous calcium chloride powder was poured into the test cup, the mouth of the test cup was sealed with composite cling film, and weighing was carried out at intervals of 12 h until the change in weight was less than 0.001 g. The water vapor permeability (WVP) was calculated using eq. (3).

$$WVP = \frac{mL}{At \cdot \Delta p} \tag{3}$$

where m is the mass of water through the membrane (g), L is the thickness of the membrane (m), A is the area of the membrane through which the water is transmitted (m^2), t is the water transmission time (s), Δp is the vapor pressure of water on both sides of the membrane (Pa).

The CDP of the films was determined by the alkali absorption method (Zhang et al., 2019) and the CDP was calculated using eq. (4).

$$\mathrm{CDP} = \frac{\mathrm{m}\,L}{\mathrm{At} \cdot \Delta P} \tag{4}$$

where: CDP-Carbon dioxide transmission rate, %; m-Mass of CO_2 through the membrane, g; L-Thickness of the membrane, mm; A-Transmission of water through the membrane area, m^2; t-Moisture transmission time, s; ΔP ΔP-vapor pressure of moisture on both sides of the membrane, Pa.

Adopting agar diffusion technology, drug diffusion in agar inhibits the growth of the surrounding indicator bacteria to form a bacterial inhibition circle, according to the size of the inhibition circle to determine the antimicrobial activity (Mittal et al., 2021).

2.4.7. Surface contact angle measurement (WCA)

The contact angles of four groups of membranes were measured using static contact angle measurements.

2.4.8. Antioxidant capacity

Determination of antioxidant properties of membrane samples, including DPPH radical scavenging rate and ABTS radical scavenging rate.

The DPPH scavenging activity (RSADPPH) of membrane samples was calculated using eq. (5), based on the improved method of DPPH determination by Marinova et al.(Marinova & Batchvarov, 2011).

$$\mathrm{RSA}_{DPPH}(\%) = \frac{A_0 - A_1}{A_0} \times 100 \tag{5}$$

where: A_0 is the absorbance after the reaction of the blank group; A_1 is the absorbance after the reaction of the membrane sample solution.

The ABTS radical scavenging assay method was improved according to Zhou et al.(Zhou et al., 2019), and the ABTS radical scavenging activity (RSAABTS) of membrane samples was calculated using eq. (6).

$$\mathrm{RSA}_{ABTS}(\%) = \frac{A_0 - A_1}{A_0} \times 100 \tag{6}$$

The above two sets of experiments were done three times in parallel, and the values measured were averaged.

2.5. Preservation performance of composite films on Actinidia arguta

2.5.1. Actinidia arguta coating treatment (light vs. dark conditions)

Actinidia arguta fruits of uniform size and ripeness were selected and randomly divided into six groups, with ten fruits per group: Light-exposed control group (Blank-S); Dark control group (Blank-P); Chitosan-coated, light-exposed group; Chitosan-coated, dark group; CSTD-coated, light-exposed group; CSTD-coated, dark group (CSTD-P). The fruits in the CS-S, CS-P, CSTD-S, and CSTD-P groups were wrapped with CS or CSTD films, while the Blank groups were left untreated. The light-exposed groups were stored under 1500 lx illumination with a 12-h light/dark cycle at 4 °C and 80 % humidity. Dark groups were placed in dark chambers covered with lightproof cloth under identical temperature and humidity conditions. Samples were analyzed on days 0, 2, 4, 6, 8, and 10, with three replicates per measurement.

2.5.2. Determination of weight loss and hardness of Actinidia arguta during preservation by different treatments

Weight loss was determined by measuring the mass of fruit before and after storage, three parallel test groups were set up for each set of samples and weighed, *Actinidia arguta* weight loss rate was calculated using eq. (7).

$$WL = \frac{m_0 - m_1}{m_0} \times 100\% \tag{7}$$

where m_0 is the initial mass, and m_1 is the final mass.

The fruit hardness of three *Actinidia arguta* species of similar size and shape was determined at three points selected at the equator using a texture meter.

2.5.3. Determination of decay rate and colony size of Actinidia arguta during preservation by different treatments

25 g of the sample was placed in a sterile cup containing 225 mL of phosphate buffer, homogenized, and left to incubate for 24 h. Bacterial growth and changes in the morphology of the organisms were observed, and the total number of colonies was calculated using eq. (8).

$$N = \frac{\sum C}{(n_1 + 0.1 \times n_2) \times d} \tag{8}$$

where $\sum C$ is the sum of the number of colonies in the plates (plates containing the appropriate range of colony numbers), n_1 is the number of plates at the first dilution (low dilution), n_2 is the number of plates at the second dilution (high dilution), and d is the dilution factor (first dilution).

The decay rate was determined following the method described by Zhao et al. (Zhao Wang et al., 2023). The decay rate is calculated using eq. (9).

$$Decay\ rate = \sum \frac{Decay\ level \times Number\ of\ fruits\ of\ this\ level}{Highest\ decay\ level \times Total\ number\ of\ fruits} \tag{9}$$

2.5.4. Determination of respiratory intensity and soluble solids (TSS) during preservation of Actinidia arguta

Actinidia arguta respiration intensity was determined using the stationary method and calculated using eq. (10).

$$Breathing\ intensity = \frac{(V_2 - V_1) \times c \times 44}{m \times h} \tag{10}$$

where V_1 is the blank titration volume (mL), V_2 is the sample titration volume (mL), c is the concentration of oxalic acid (mol/L), m is the mass of the sample (kg), and h is the measurement time.

Two drops of *Actinidia arguta* juice were added to the surface of the prism of an Abbe refractometer, and the soluble solids content was observed and measured.

2.5.5. Actinidia arguta VC content and, titratable acid (TA) determination during freshness preservation

The content of VC in *Actinidia arguta* was analyzed by the 2,6-dichloroindophenol method and the content of VC in *Actinidia arguta* was calculated using eq. (11).

$$VC = \frac{V \times (V_1 - V_0) \times \rho}{m \times V_2} \times 100 \tag{11}$$

where V is the total volume of *Actinidia arguta* extract (mL), V_1 is the volume of 2,6-dichloroindophenol consumed in the titration of *Actinidia arguta* (mL), V_0 is the volume of 2,6-dichloroindophenol consumed in the titration of oxalic acid (mL), and ρ is the mass of VC equivalent to 1 mL of 2,6-dichloroindophenol (mg/mL); V_2 is the volume of the sample extract (mL), and m is the mass of *Actinidia arguta* (g). volume of sample extract (mL), m is the mass of *Actinidia arguta* (g).

5 g of ground *Actinidia arguta* tissue was diluted to 50 mL using distilled water, and the titratable acid determination of the *Actinidia arguta* mixture was carried out by using the international standard ISO 750-1981, and the formula was calculated using eq. (12).

$$TA = \frac{KCV_3 \times V_1 \times 100}{WV_2} \tag{12}$$

where W is the weight of the sample (g), C is the concentration of NaOH (0.1 mol/L), V_1 is the total sample during extraction (mL), V_2 is the amount of the sample during measurement (mL), and V_3 is the amount of NaOH consumed (mL). k is the conversion factor: in terms of the total number of acids, the conversion factor is 0.070.

2.5.6. Determination of antioxidant capacity of Actinidia arguta during the preservation period

Determination of DPPH and ABTS radical scavenging in *Actinidia arguta* as in 2.4.8.

2.5.7. Enzyme activity content of Actinidia arguta during freshness preservation

Superoxide dismutase (SOD) and peroxidase (POD) were determined using the Beijing Solaybao Technology Co., Ltd. Solaybao micro assay kit, which is based on the principle of a specific chemical reaction to quantify the enzyme activities in *Actinidia arguta* samples.

2.5.8. Determination of malondialdehyde (MDA), total phenols (TPC), and total flavonoids (TFC) in peach by Actinidia arguta during the preservation period

The OD values at 532 nm and 450 nm were determined using the clear night method in accordance with the national food safety standard GB5009.181–2016, and the MDA content in *Actinidia arguta* was calculated using eq. (13).

$$C = 6.45OD_{532} - 0.56OD_{450} \tag{13}$$

The standard curve of different concentrations of gallic acid standard phenol solution was plotted, the sample was taken and added with 80 % methanol, sonicated for 30 min, centrifuged at 4000 rpm for 10 min, 1 mL of the supernatant was taken, 5 mL of forskolin-phenol reagent was added, and 4 mL of 7.5 % sodium carbonate was added after 5 min of resting time, and then mixed well, and then placed in the dark place for 30 min for the determination of OD value of 765 nm, and then the total phenol content of the samples was calculated according to the standard curve. The total phenol content of the sample was calculated according to the standard curve.

Plot the curve of different concentrations of standard flavonoid solution, take the sample and add 80 % methanol, ultrasonic 30 min, centrifugation at 4000 rpm for 10 min, take 1 mL of supernatant, add 0.3 mL 5 % $NaNO_2$, let it stand for 5 min, add 0.3 mL of 10 % $AlCl_3$ solution, let it stand for 6 min, add 2 mL of 1 M NaOH solution, and fix it to 10 mL with distilled water. After mixing, determine the OD value at 510 nm, and calculate the total flavonoid content of the sample according to the standard curve.

3. Results and analysis

3.1. Measurement results of physical and chemical indexes of the composite membrane

3.1.1. FT-IR results

The Fourier-transform infrared (FT-IR) spectra of the composite films are presented in Fig. 2(A). The characteristic functional groups were identified based on the literature(Jovanović et al., 2021). A broad O—H stretching band at 3396 cm^{-1} in CSD, CST, and CSTD films indicates increased hydroxyl group content and stronger hydrogen bonding due to DEO and nano-TiO_2 incorporation. The C—H stretching vibration at 2811 cm^{-1} shows enhanced intensity in CSD and CSTD films, while the

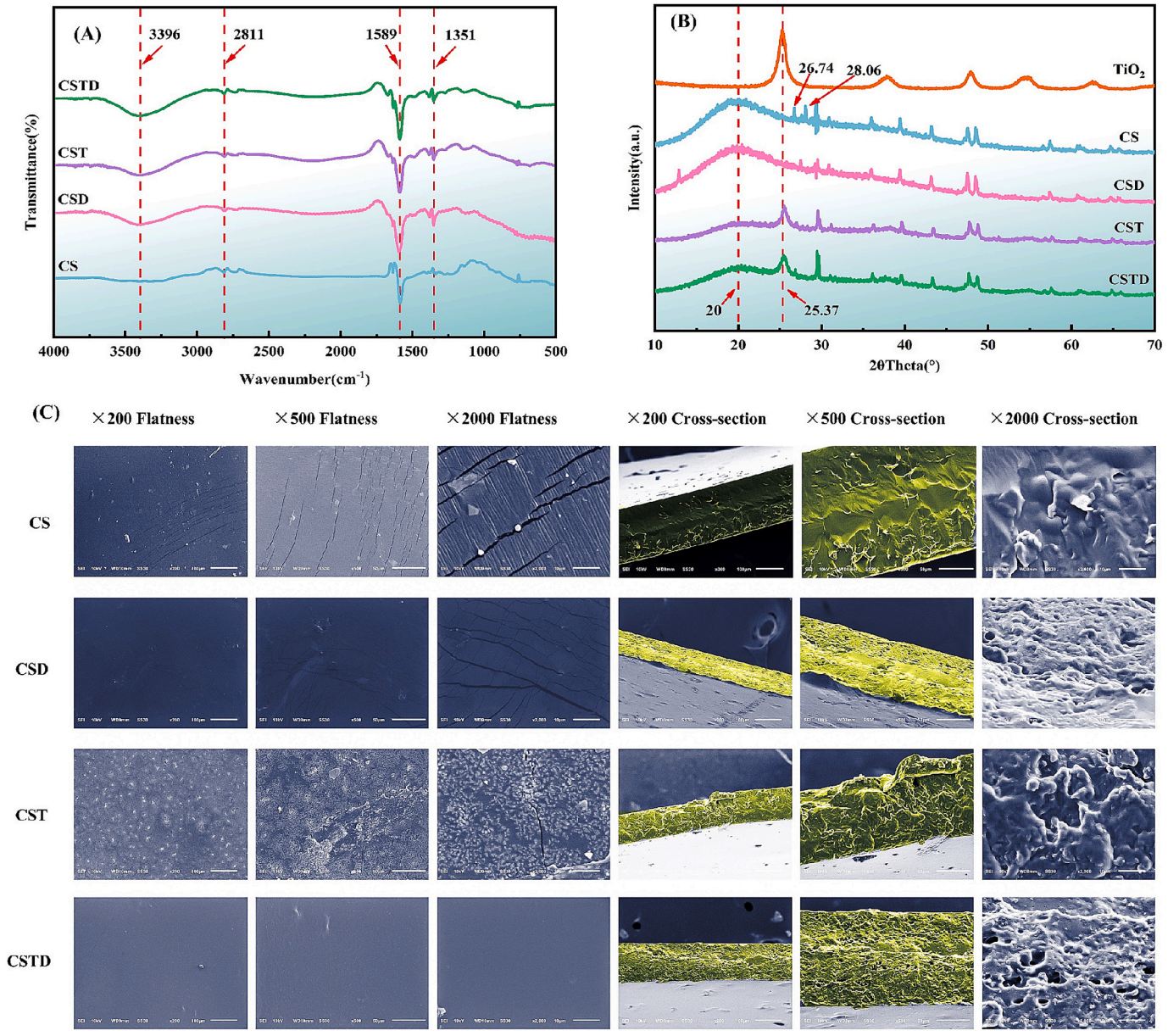

Fig. 2. (A) FT-IR Analysis of composite films;(B) XRD analysis of composite films;(C) SEM analysis of composite films.

C—N stretching vibration at 1351 cm^{-1} suggests molecular adjustments. A peak at 1589 cm^{-1}, linked to C═O stretching, implies the formation of esters or carboxylic acids, These observations align with those reported by Zahra et al.(Soltani, Tavakolipour, & Tabari, 2023) who observed similar shifts in the FT-IR spectra of poly(lactic acid) films combined with chitosan and nano-TiO_2. These shifts indicate cross-linking among CS, DEO, and nano-TiO_2, strengthening the hydrogen bonding network and enhancing the films' mechanical stability and performance.

3.1.2. XRD results

The XRD results are shown in Fig. 2(B), CS and CSD showed strong diffraction peaks near 20°(Liu Cai, Sheng, Ma, Xu, & Jin, 2019), indicating the presence of amorphous or amorphous structure of CS attributed to crystal II. CST and CSTD showed a significant decrease in peak intensity at 20° and became wider after the addition of nano-TiO_2, and a strong peak appeared at 25.37°, which may be due to the molecular movement of CS and nano-TiO_2 restriction, molecular interactions were formed, suggesting that cross-linking occurred during the film formation process between CS and nanoTiO_2 and a relatively amorphous complex was formed. While the weak peaks of CS at 26.74° and 28.06° only existed in one place in CSD and disappeared in CST and CSTD indicating that the incorporation of DEO and nanoTiO_2 disrupted the intermolecular hydrogen bonding of CS, which led to the intertwining of the molecular chains of CS, DEO, and nanoTiO_2, resulting in the reduction of the crystal structure, which produced the change of the mechanical and physical properties and the formation of a more stable composite Structure. In the CS/*Moringa oleifera* gum/nano silicon dioxide composite membrane prepared by Ruby et al.(Thomas, Prabha, Sanuja, & Umapathy, 2023), the XRD of the CS peak at 22° became less sharp and wider with the addition of nano silicon dioxide, indicating the successful incorporation of nanoparticles into the framework of the composite film.

3.1.3. SEM analysis

The SEM Fig. 2(C) reveals that the CS membrane has obvious cracks and a tight cross-section, and a small number of CS particles were found to be undissolved at ×2000, and the appearance of cracks affects the mechanical properties of the membrane. Adding DEO reduced cracks, eliminated CS particle precipitation, and introduced fine cavities in the

cross-section, likely due to DEO-CS cross-linking. When CS was combined with nano TiO_2, there were no obvious cracks on the surface, only a crack was observed at ×2000, a large number of white agglomerated particles appeared on the surface, which were nano TiO_2, at the same time, there were a small number of CS particles precipitated, no cavities appeared on the cross-section, TiO_2 particles could be observed, which indicated that the nano TiO_2 was well dispersed in the CST membrane. The CSTD membrane exhibited a smooth, dense structure with no cracks, cavities, or particle precipitation, attributed to DEO and nano-TiO_2 cross-linking. With no particle precipitation and no cracks, the cross-section is observed to have a dense structure with a small number of microscopic cavities, which reduces the roughness and porosity of the membrane. Combined with the SEM analysis of CSD and CST, the cross-section cavities are due to the addition of DEO, which may be due to the hydrophobicity of DEO, while the addition of nano-TiO_2 reduces the cavities, which enhances the polymer-polymer interactions. A similar phenomenon was obtained in the study of CS/whey isolate protein active film containing TiO_2 and white pepper essential oil by Wang et al. (Wang et al., 2022), while nano-TiO_2 enhanced density in CS-based films. The interaction among CS, DEO, and nano-TiO_2 forms a homogeneous, dense network, reflected in differences observed in the physical properties (Sections 3.1.6 and 3.1.7).

3.1.4. Thermogravimetric analysis (TGA) results

The thermogravimetric analysis (TGA) results for the CS and composite films are shown in Figs. 3(A) and 3(B). The first stage (30–176 °C) involves moisture evaporation with stable heat flow. As illustrated in Fig. 3(B), the heat flow remained relatively stable during this stage, indicating a dynamic equilibrium associated with the removal of adsorbed moisture or volatile substances. In the second stage (176–268 °C), the CSTD film showed lower weight loss than CS, CSD, and CST films due to its distinct composition. The fluctuations in the heat flow curve suggest that this stage corresponds to the release of volatile components or adjustments in the adsorption-desorption equilibrium within the samples. Between 268 and 363 °C, weight loss differences became more pronounced; DEO and nano-TiO_2 slowed degradation in composite films, while CS degraded rapidly. Above 363 °C, all films showed accelerated weight loss, with CS losing the most and CSTD the least. This behavior may be associated with more complex decomposition reactions or further breakdown of degradation products. The continuous downward trend in the heat flow curve at elevated temperatures suggests that the organic or polymeric components began to degrade into low-molecular-weight products, involving the cleavage of chemical bonds and the release of gases or other by-products. The FT-IR and XRD results further support the conclusion that cross-linking interactions occurred among CS, DEO, and nano-TiO_2, enhancing the stability of the composite films. These interactions increased the interchain bonding, creating a more stable network. Similar findings were reported by Ahmed et al. (Youssef, El-Sayed, El-Sayed, Fouly, & El-Aziz, 2023), where the addition of nano-TiO_2 and essential oils shifted the TGA curve to higher temperatures, reaching 403 °C. This indicates that the inclusion of nano-TiO_2 and bioactive compounds effectively enhances the thermal stability of the composite films, making them more resistant to thermal degradation. In summary, the CSTD film demonstrated superior thermal stability compared to the CS, CSD, and CST films, reflecting the synergistic effect of nano-TiO_2 and DEO in

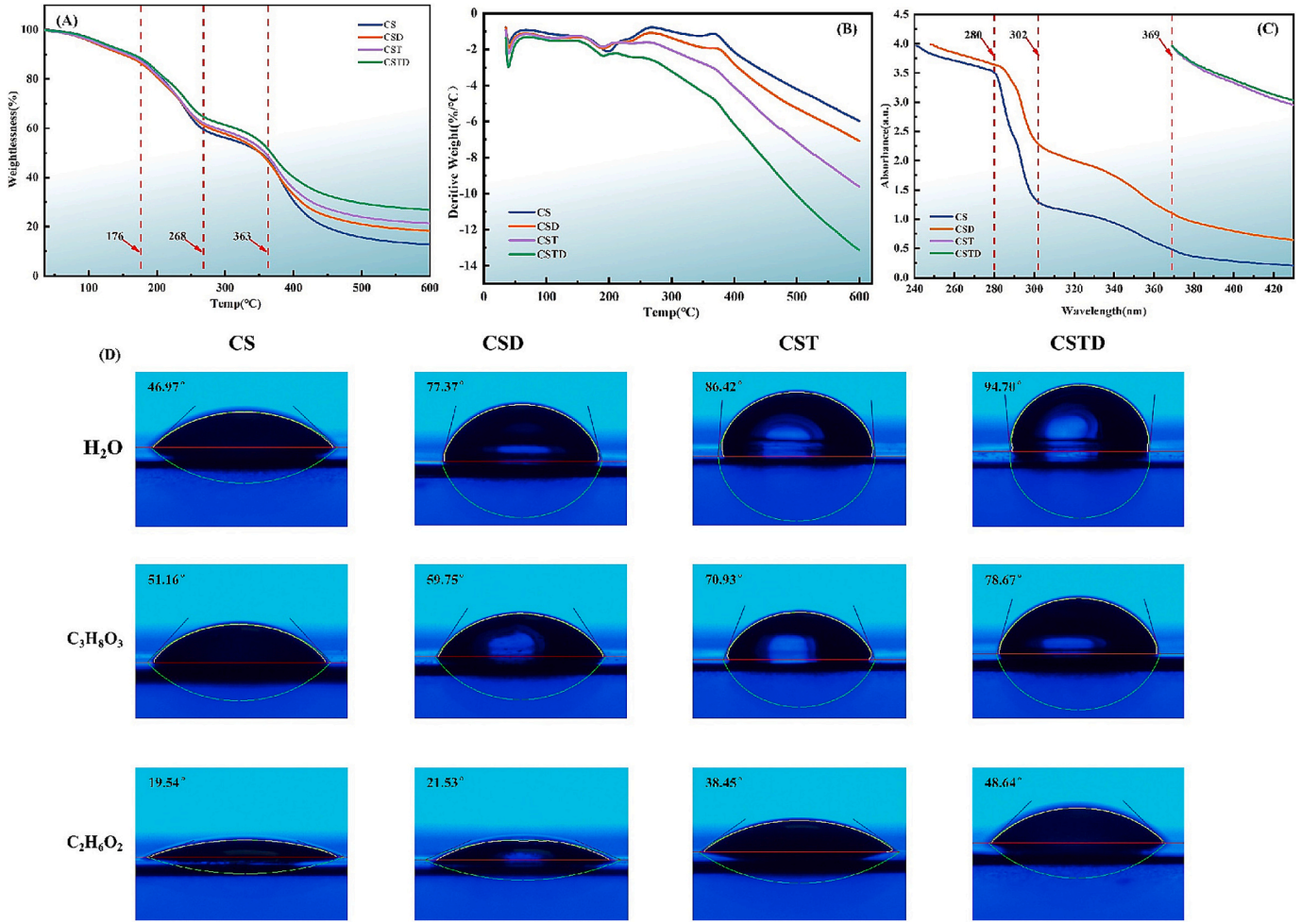

Fig. 3. (A, B)TGA analysis of composite films;(C) UV–visible analysis of composite films;(D) WCA analysis of composite films.

improving the film's resistance to decomposition. This enhanced thermal performance makes the CSTD film a suitable candidate for applications that require robust thermal stability.

3.1.5. UV–visible spectroscopy results and analysis

The UV–Visible absorbance spectra of the composite films are shown in Fig. 3(C). Significant differences in UV-blocking capabilities were observed among the four types of films. The pure CS film exhibited low absorbance across the UV spectrum, indicating limited UV-blocking ability. The CSD film showed similar UV transmittance to the CS film up to 280 nm, with a slight increase in absorbance beyond 302 nm, likely due to the UV-absorbing properties of compounds present in the DEO. The CST and CSTD films, containing nano-TiO_2, demonstrated a significant enhancement in UV absorption, with absorbance peaks appearing at 369 nm and beyond. The combination of DEO and nano-TiO_2 in the CSTD film resulted in the highest absorbance across the UV spectrum, indicating superior UV-blocking performance due to the synergistic interaction between the components. This finding aligns with previous research by Yuan et al. (Xue et al., 2023), which reported that incorporating essential oils and nano-TiO_2 into chitosan films significantly reduced UV transmittance, with values below 10 % or even 0 % throughout the UV range. UV radiation induces photochemical reactions that are detrimental to food quality, especially for light-sensitive products. The CSTD film's strong UV-blocking ability suggests its potential application in food preservation by preventing UV-induced photodegradation, thus extending storage life.

3.1.6. WCA results and analysis

The WCA results (Fig. 3D) show notable hydrophobicity differences among the films. The CS film had the lowest contact angle, indicating poor hydrophobicity and limited moisture barrier properties. The addition of DEO improved the hydrophobicity of the CSD film, as the hydrophobic compounds in DEO repelled water molecules, resulting in an increased contact angle. The CST film further enhanced hydrophobicity with the incorporation of nano-TiO_2, which improved resistance to liquid permeation and strengthened the barrier properties. The CSTD film exhibited the highest contact angle (94.70°), surpassing the 90° threshold for hydrophobicity, indicating superior liquid barrier performance. This improvement is attributed to the synergistic interaction among CS, DEO, and nano-TiO_2, which formed a microstructured surface capable of trapping air pockets and keeping water droplets suspended on the surface. These findings align with the study by Liu et al. (Liu et al., 2021), which demonstrated that the incorporation of essential oils and titanium dioxide nanoparticles into chitosan-based films significantly improved their hydrophobicity. The excellent hydrophobicity of the CSTD film effectively prevents moisture absorption, inhibits microbial growth, and maintains the quality of packaged food during extended storage periods.

3.1.7. Physical and antibacterial properties of composite films

The physical properties and antibacterial performance of the composite films are summarized in Table 1. Under comparable thickness, the tensile strength (TS) was significantly improved in CST and CSTD films, indicating that the addition of nano-TiO_2 effectively enhanced the mechanical properties. However, both DEO and nano-TiO_2 reduced the elongation at break (EAB) values, suggesting that the interaction between components increased molecular cohesion and network formation, thus reinforcing the durability and resistance of the films to mechanical damage. This makes the films suitable for food packaging, ensuring easier handling, transportation, and storage. In terms of water vapor permeability (WVP), the CSTD film exhibited the lowest value (0.802 ± 0.010 g·mm·cm^{-2}·h^{-1}·kPa^{-1}), indicating superior moisture resistance. This result, combined with the WCA analysis, suggests that the CSTD film can effectively prevent water infiltration, thereby inhibiting microbial growth and delaying food spoilage. The CO_2 permeability (CDP) values revealed that the CS film had the lowest gas permeability

Table 1
Physical properties and antibacterial performance of composite films.

		CS	CSD	CST	CSTD
TS (Mpa)		$6.428^{c} \pm 0.233$	$4.785^{d} \pm 0.262$	$14.653^{a} \pm 0.187$	$14.190^{b} \pm 0.131$
EAB (%)		$44.366^{a} \pm 2.228$	$38.583^{b} \pm 1.916$	$35.743^{b} \pm 1.545$	$36.635^{b} \pm 2.174$
Thicknesses (mm)		$0.162^{a} \pm 0.015$	$0.164^{a} \pm 0.011$	$0.180^{a} \pm 0.014$	$0.171^{a} \pm 0.011$
WVP (g·mm·cm^{-2}·h^{-1}·Kpa^{-1})		$0.939^{a} \pm 0.021$	$0.911^{a} \pm 0.015$	$0.882^{b} \pm 0.012$	$0.802^{c} \pm 0.010$
CDP (g·mm·cm^{-2}·h^{-1}·Kpa^{-1})		$0.010^{c} \pm 0.002$	$0.018^{b} \pm 0.001$	$0.048^{b} \pm 0.002$	$0.060^{a} \pm 0.001$
Antimicrobial properties (mm)	***E. coli***	$11.363^{d} \pm 0.544$	$17.851^{c} \pm 0.753$	$22.593^{b} \pm 0.871$	$25.842^{a} \pm 0.731$
	S. aureus	$13.784^{d} \pm 0.524$	$18.461^{c} \pm 0.431$	$21.573^{b} \pm 0.462$	$26.631^{a} \pm 0.410$

(0.010 ± 0.002 g·mm·cm^{-2}·h^{-1}·kPa^{-1}). Although DEO had a negligible effect on gas permeability, the incorporation of nano-TiO_2 significantly increased CDP, with the CSTD film reaching 0.060 ± 0.001 g·mm·cm^{-2}·h^{-1}·kPa^{-1}. This suggests that CSTD films offer enhanced gas barrier properties, helping regulate gas exchange and maintain the freshness of packaged foods. The antibacterial performance, measured by inhibition zones against *Escherichia coli* and *Staphylococcus aureus*, revealed significant improvements in CST and CSTD films. The CST film achieved inhibition zones of 22.593 ± 0.871 mm for *E. coli* and 21.573 ± 0.462 mm for *S. aureus*. The CSTD film exhibited the highest antibacterial activity, with inhibition zones of 25.842 ± 0.731 mm for *E. coli* and 26.631 ± 0.410 mm for *S. aureus*, demonstrating the synergistic effect of DEO and nano-TiO_2 in enhancing antimicrobial properties. The superior antibacterial activity of the CSTD film can be attributed to the photocatalytic activity of nano-TiO_2, which generates reactive oxygen species under UV light, leading to the inactivation of microorganisms. Additionally, the bioactive compounds in DEO further enhance antimicrobial efficacy.

In the study by Chang et al. (Chang et al., 2021), CS/glyceryl laurate/nano-TiO_2 composite membranes. With similar thickness, the introduction of nano TiO_2 increased the TS of the composite film and decreased the EAB, while the addition of nano TiO_2 to the composite film exhibited lower WVP and CDP compared to CS, suggesting that TiO_2 enhances the network structure of the film and increases the film cohesion. Gohargani et al. (Gohargani, Lashkari, & Shirazinejad, 2020) reported that the TS of the films increased with the addition of nano TiO_2 alone, but significantly decreased with the addition of nano TiO_2 and Zataria multiflora essential oil. Dong et al.(Dong, Li, & Gong, 2021) prepared CS/nano TiO_2/nano silver composite films against *E. coli* with inhibitory circle diameters of up to 22 mm, CS of 16.17 mm, and for *S. aureus* the diameter of the circle of inhibition was 16.17 mm for CS and 16.33 mm for the composite film, indicating that the composite film could enhance the antimicrobial activity of *E. coli* and *S. aureus*.

3.1.8. Antioxidant capacity results and analysis

The antioxidant properties of the composite films were evaluated using the radical scavenging activity (RSA) assays for hydroxyl radicals, DPPH, ABTS, and superoxide anions. The results, presented in Fig. 4, highlight the significant differences in the antioxidant capacity among the different film types. DPPH Radical Scavenging: In Fig. 4(A), the CSTD film demonstrated the strongest DPPH radical scavenging ability, achieving a clearance rate of 89.65 %. This superior performance indicates a high level of antioxidant potential, primarily attributed to the phenolic compounds in DEO. ABTS Radical Scavenging: Fig. 4(B) shows that the ABTS clearance rate for the CSTD film reached 87.86 %, confirming its effectiveness in neutralizing ABTS radicals. The enhanced antioxidant capacity of the CSTD film can be attributed to the synergy between DEO and nano-TiO_2. The phenolic and terpenoid compounds in DEO act as effective free radical scavengers, while the photocatalytic

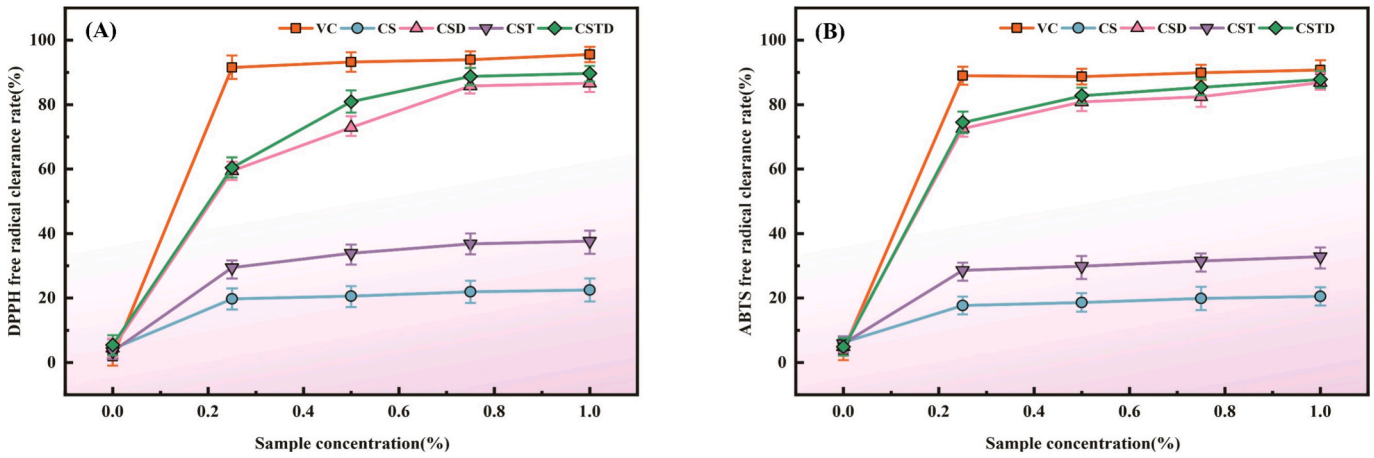

Fig. 4. Antioxidant capacity of composite films: (A) DPPH free radical clearance rate; (B) ABTS free radical clearance rate.

activity of nano-TiO_2 further enhances the film's ability to combat reactive oxygen species (ROS). These results are consistent with the findings of Swarup et al. (Roy et al., 2021), who reported that chitosan-based films with TiO_2 nanoparticles and bioactive compounds exhibited superior antioxidant performance. In summary, the high antioxidant activity of the CSTD film indicates its potential to protect food products from oxidative degradation, extending shelf life and preserving nutritional quality.

3.2. Preservation effects on Actinidia arguta

3.2.1. Weight loss and firmness

The weight loss and firmness of *Actinidia arguta* during storage under various treatments are shown in Figs. 5(B) and 5(C). On day 10, the Blank-S group exhibited the highest weight loss at 69.34 %, followed by the Blank-P group at 63.66 %. The CS-S and CS-P groups showed moderate weight loss, at 56.84 % and 52.84 %, respectively. In contrast, the CSTD-S and CSTD-P groups demonstrated the lowest weight loss, with values of 18.68 % and 18.26 %, respectively. These results indicate that the CSTD film effectively minimized moisture loss, significantly outperforming the other treatments. Firmness measurements further confirmed the efficacy of the CSTD films. As shown in Fig. 5(C), fruits treated with CSTD films maintained the highest firmness throughout the storage period. On day 10, the CSTD-P group exhibited a firmness of 23.54 N, nearly three times that of the Blank-S group (7.89 N). These results suggest that the CSTD film successfully preserved the structural integrity of the fruit, preventing excessive softening and extending its shelf life. The superior performance of the CSTD film can be attributed to its excellent moisture barrier properties, which reduce water loss and delay texture degradation. Similar results were reported by Wang et al. (Wang Yang et al., 2022), where essential oil-enriched chitosan films significantly reduced weight loss and preserved the firmness of mangoes during storage.

3.2.2. Analysis of decay rate and total microbial count in Actinidia arguta under different treatments during storage

As shown in Fig. 5(A), the appearance changes of *Actinidia arguta* during the preservation period by different treatments, *Actinidia arguta* was preserved by wrapping with composite film, and photographs were taken after removing the composite film on the rest of the days except the 0th d. The Blank group started to show yellowing on the 5th d under the light condition, and molds started to grow on the 6th d. The CS group started to show partial yellowing on the 7th d, and the CSTD group always remained relatively fresh for 10 d. The difference between CSTD-S and CSTD-P status was also found in Fig. 5(A). The CS group began to show partial yellowing on the 7th d. The CSTD group remained relatively fresh throughout the 10 d and there was little difference between the CSTD-S and CSTD-P status. The decay rate and microbial count of

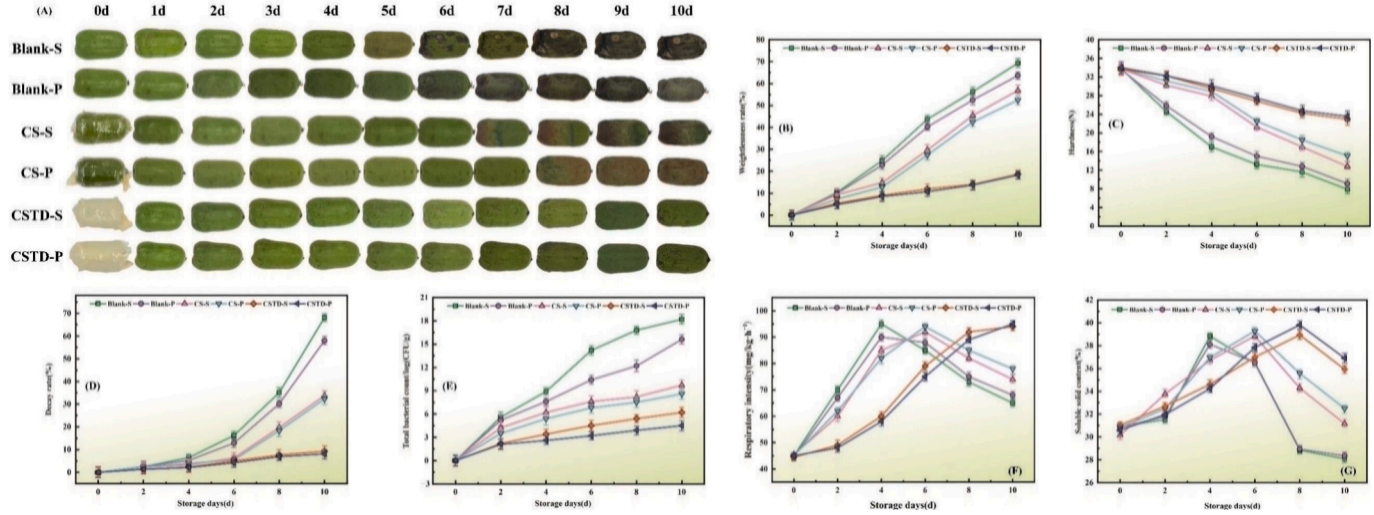

Fig. 5. (A) Appearance changes of *Actinidia arguta*; (B) weight loss rate of *Actinidia arguta*; (C) firmness of *Actinidia arguta*; (D) decay rate of *Actinidia arguta*; (E) total bacterial count of *Actinidia arguta*; (F) respiration intensity of *Actinidia arguta*; (G) TSS of *Actinidia arguta*.

Actinidia arguta under different treatments are presented in Figs. 5(D) and 5(E). On day 10, the highest decay rate was observed in the Blank-S group, reaching 68.18 %, followed by the Blank-P group at 58.04 %. The CS-S and CS-P groups exhibited moderate decay rates of 33.72 % and 32.37 %, respectively. In contrast, the CSTD-S and CSTD-P groups showed significantly lower decay rates, at 9.3 % and 8.1 %, respectively, indicating that the CSTD films effectively suppressed fruit spoilage. The microbial count analysis showed a similar trend. On day 10, the Blank-S group had the highest microbial count at 18.2 CFU/g, with the Blank-P group following at 15.7 CFU/g. The CS-S and CS-P groups exhibited microbial counts of 12.8 CFU/g and 10.5 CFU/g, respectively. The lowest microbial counts were observed in the CSTD-S and CSTD-P groups, at 6.2 CFU/g and 4.5 CFU/g, respectively. These results demonstrate that the application of CSTD films significantly reduces both decay and microbial proliferation. The improved antimicrobial performance is attributed to the combined effect of nano-TiO_2 and DEO. Nano-TiO_2, through its photocatalytic properties, generates reactive oxygen species that disrupt microbial cells, while the bioactive compounds in DEO enhance the antibacterial effect. This synergistic interaction helps inhibit the growth of spoilage organisms, extending the shelf life of *Actinidia arguta* under both light and dark storage conditions. Xing et al.(Xing et al., 2021) used CS as a substrate to add salicylic acid and nano TiO_2 to prepare a composite membrane to explore the effect on the storage quality of blackcurrant berries, achieved results consistent with this paper, the composite membrane effectively inhibited the growth of bacteria, and proposed that the composite membrane prepared with nano TiO_2 as an outer membrane protective barrier, which can kill or harm bacterial colonies, preventing or slowing down the entry of bacteria into blackcurrant fruits.

3.2.3. Respiration rate and TSS

The respiration rate and TSS content of *Actinidia arguta* under different treatments are presented in Figs. 5(F) and 5(G). The respiration rate reflects the metabolic activity of the fruit, which accelerates ripening and deterioration. As shown in Fig. 5(F), the Blank group exhibited a rapid increase in respiration rate, peaking on day 4 (95 mg/kg·h^{-1}), followed by a sharp decline. The light-exposed groups demonstrated higher respiration rates compared to the dark-stored ones, indicating that exposure to light accelerates metabolic processes. In contrast, the respiration rates of the CS-treated groups (CS-S and CS-P) peaked on day 6 (92–94 mg/kg·h^{-1}). Meanwhile, the CSTD-treated groups (CSTD-S and CSTD-P) exhibited a more gradual increase in respiration rates, reaching stable levels of 94 mg/kg·h^{-1} and 95 mg/kg·h^{-1}, respectively, by the end of storage. The CSTD films effectively suppressed excessive respiration, with no significant difference between the light and dark storage conditions. This moderation in respiration rate helps to extend the shelf life of the fruit by slowing the ripening process. These results suggest that nano-TiO_2 in the CSTD films plays a crucial role in regulating the fruit's respiration. By blocking UV radiation, the films reduce light-induced oxidation, minimizing metabolic stress. Similar findings were reported by Xing et al. (Xing et al., 2020), where chitosan/nano-TiO_2 films were used to preserve mango fruits, demonstrating a delayed peak in respiration rate compared to untreated samples. The TSS content, which reflects the sugar and soluble solids levels, is another critical indicator of fruit quality. As shown in Fig. 5(G), the TSS levels in the Blank groups peaked on day 4 but dropped rapidly thereafter, indicating a loss of sugars during storage. The CS-treated groups peaked on day 6, showing a slight delay in sugar loss compared to the Blank groups. In the CSTD-treated groups, however, the TSS levels peaked on day 8, with CSTD-P and CSTD-S maintaining TSS values of 36.90 % and 35.92 %, respectively, by day 10. The ability of the CSTD films to maintain higher TSS levels suggests their effectiveness in slowing down sugar degradation, thus preserving the fruit's flavor and sweetness throughout storage. The structural integrity and gas barrier properties of the CSTD films likely contribute to the stabilization of the fruit's internal environment, reducing oxidative degradation and water loss. These findings are consistent with a study by Li et al., which showed that chitosan-based films containing tea polyphenol nanoparticles effectively delayed the degradation of TSS in strawberries during storage(Li Hua et al., 2024). The results highlight the potential of CSTD films to regulate the fruit's gas exchange, maintain optimal oxygen and carbon dioxide levels, and reduce water evaporation, thus preserving the quality of *Actinidia arguta* for an extended period.

3.2.4. VC and TA

The changes in VC content and titratable acidity (TA) of *Actinidia arguta* under different treatments are presented in Figs. 6(A) and 6(B). VC content is a key indicator of nutritional quality, as it degrades easily during storage due to oxidation. As shown in Fig. 6(A), the VC content in the Blank-S group decreased rapidly, with only 38.45 % of the initial content retained by day 10. The Blank-P group performed slightly better, with a retention rate of 42.77 %. The CS-treated groups (CS-S and CS-P) exhibited moderate retention, maintaining 64.29 % and 68.34 % of their initial VC content by day 10, respectively. In contrast, the CSTD films significantly delayed VC degradation. The CSTD-P and CSTD-S groups retained 85.32 % and 82.67 % of their original VC content, respectively, by the end of storage. The enhanced preservation of VC in the CSTD-treated fruits can be attributed to the film's antioxidant properties, which limit oxidative reactions(Petriccione et al., 2015). The superior VC retention in the CSTD films aligns with findings from previous studies, where composite films containing essential oils and nanoparticles effectively reduced oxidation-induced nutrient loss during storage(Li Zhou, Wang, Cai, Yue, & Cui, 2021). This result suggests that the CSTD films provide a protective barrier that stabilizes the internal environment of the fruit, minimizing VC degradation. Fig. 6(B) presents the TA changes, which reflect the fruit's acidity and influence its sensory quality. In the Blank groups, TA levels decreased sharply during storage, indicating that organic acids were consumed during metabolic processes. By day 10, the TA levels in the Blank-S and Blank-P groups had decreased to 0.994 % and 1.125 %, respectively. The CS-S and CS-P groups exhibited better TA retention, with final levels of 1.01 % and 1.16 %, respectively. However, the CSTD films were the most effective at maintaining TA. The CSTD-P group retained a TA level of 1.397 % by the end of storage, while the CSTD-S group achieved 1.362 %. These results suggest that the CSTD films help to preserve acidity by limiting metabolic activity and reducing organic acid consumption. The stability of both VC and TA under CSTD treatment confirms the film's ability to create a favorable microenvironment that slows down enzymatic and oxidative processes. This not only preserves the fruit's nutritional content but also maintains its flavor and sensory appeal. The findings are consistent with previous research showing that chitosan-based films enriched with bioactive components are effective in maintaining acidity and preventing nutrient degradation during fruit storage(Wang et al., 2023).

3.2.5. Analysis of antioxidant capacity of Actinidia arguta under different treatments during storage

As shown in Fig. 6(C), the DPPH free radical clearance rate peaked at 42 % for Blank-S on day 4 and 43.5 % for Blank-P on day 6. The CS groups showed similar behavior, peaking at 43 % for CS-S and 43.8 % for CS-P on day 6. Notably, the CSTD group achieved higher clearance rates, peaking at 43.9 % for CSTD-S and 46 % for CSTD-P on day 8. This improvement is due to the high surface area and unique optical properties of nano-TiO_2, which, when integrated with CS, form a dense and uniform film structure. This structure effectively blocks oxygen and moisture from penetrating the film, thus slowing down the oxidation process. Fig. 6(D) displays the ABTS radical clearance rate, which followed an upward trend initially before decreasing across all groups. The peak clearance rates occurred on different days: day 4 for the Blank group, day 6 for the CS group, and day 8 for the CSTD group. The peak values were 56 % (Blank-S), 54 % (Blank-P), 62 % (CS-S), 59 % (CS-P), 58 % (CSTD-S), and 60 % (CSTD-P). Under both light and dark

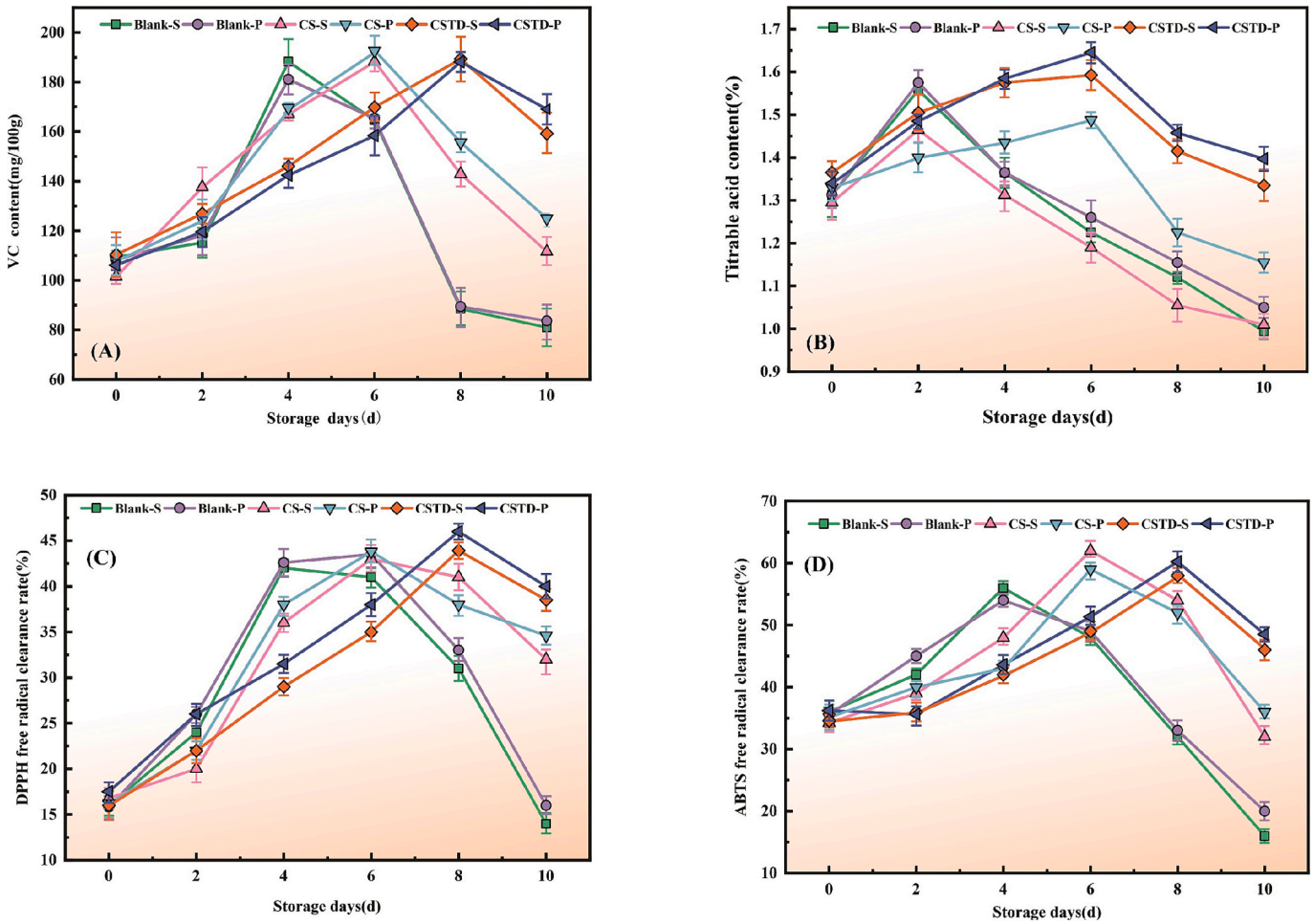

Fig. 6. (A) VC content of *Actinidia arguta*; (B) TA of *Actinidia arguta*; antioxidant activity of *Actinidia arguta*: (C) DPPH free radical clearance rate; (D) ABTS free radical clearance rate.

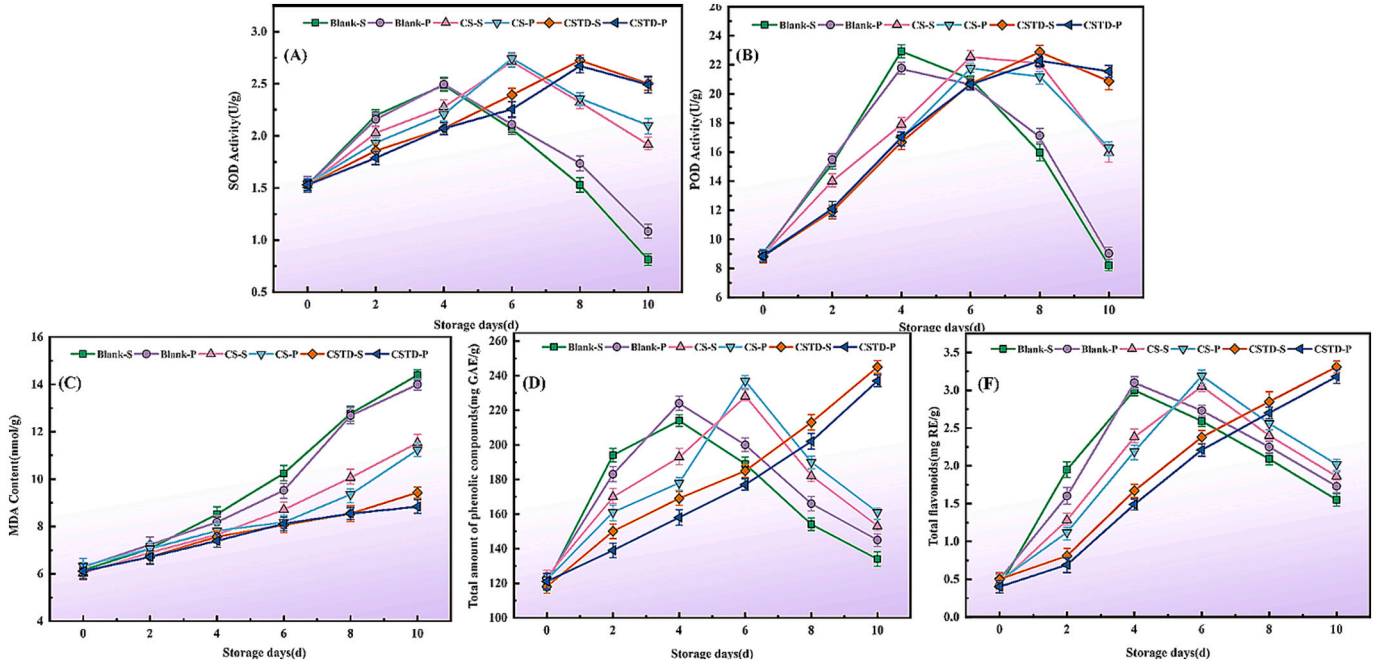

Fig. 7. Enzyme activity levels in *Actinidia arguta*: (A) SOD activity; (B) POD activity; (C) MDA content in *Actinidia arguta*; (D) TPC in *Actinidia arguta*; (F) TFC in *Actinidia arguta*.

conditions, the CSTD group exhibited enhanced ABTS clearance rates, further demonstrating the excellent UV-blocking ability of nano-TiO_2. This protection not only shields the fruit from direct UV damage but also reduces oxidative reactions caused by light exposure, thereby extending the fruit's shelf life.

These findings align with the results of Sun et al. (Sun et al., 2022), who studied a chitosan composite film with polysaccharides derived from ginseng residues. In their study, the antioxidant activity of the composite film exceeded that of single-layer films from the third day onward. By day 4, the DPPH clearance rate of the composite film was significantly higher than the control group, demonstrating its superior ability to maintain the antioxidant state of fresh-cut melon over an extended period. Similarly, Wang et al. (Zhao et al., 2023) reported that a composite film containing chitosan and Enoki mushroom stem polysaccharides effectively preserved the antioxidant properties of blueberries, with the DPPH clearance rate reaching 43.74 %, 1.16 times that of the CS group. In summary, the CSTD composite film achieves a significant improvement in free radical clearance by leveraging the biocompatibility of CS, the UV-blocking ability of nano-TiO_2, and the antioxidant properties of DEO. This synergy not only delays the oxidation process but also enhances the storage quality and prolongs the shelf life of *Actinidia arguta*.

3.2.6. Analysis of enzyme activity in Actinidia arguta under different treatments during storage

Fig. 7(A) shows the initial superoxide dismutase (SOD) activity at 1.5 U/g. The Blank group peaked on day 4, the CS group on day 6, and the CSTD group reached its maximum on day 8, with CSTD-S at 2.73 U/g and CSTD-P at 2.67 U/g. The CSTD treatment significantly enhanced SOD activity compared to the Blank and CS groups. This can be attributed to the controlled micro-oxygen environment created by the CSTD film, which inhibits the interaction between SOD and superoxide anions, thereby preserving enzyme activity. Furthermore, the film structure effectively limits oxidative stress, extending the shelf life of the fruit. Fig. 7(B) illustrates the peroxidase (POD) activity, with an initial value of 9.06 U/g. Similar to SOD, the Blank group reached its peak on day 4, the CS group on day 6, and the CSTD group peaked on day 8, with CSTD-S at 22.88 U/g and CSTD-P at 22.28 U/g. The enhanced POD activity in the CSTD group is attributed to the dense nano-porous structure formed by the interaction of CS, nano-TiO_2, and DEO. This structure regulates gas exchange and shields the enzymes from environmental stressors, such as excessive oxygen exposure and intense light, which preserves enzyme stability and activity(Sami et al., 2021).

These results align with findings by Song et al. (Song et al., 2016), who reported that incorporating nano-silica with chitosan improved the preservation of loquat fruit. In that study, SOD activity remained higher in the composite film group than in the control group throughout the 10 to 40-day storage period. Similarly, in Tian et al.'s (Tian et al., 2019) study on ginkgo seed preservation using CS/nano-TiO_2 films, the activities of SOD, CAT, and POD were consistently higher in the composite film group compared to the CS and Blank groups. In conclusion, the CSTD film effectively regulates moisture and gas exchange, while its microstructure and nano-scale properties enhance enzyme stability and activity. The synergistic effects among CS, nano-TiO_2, and DEO allow the film to maintain higher enzyme activities, thereby delaying fruit aging and extending the shelf life of *Actinidia arguta*.

3.2.7. Analysis of MDA, TPC and TFC content in Actinidia arguta under different treatments during storage

Fig. 7(C) presents the changes in malondialdehyde (MDA) content, which steadily increased over time from an initial value of 7.07 nmol/g. Compared to the Blank group, the CS group exhibited a slower rise in MDA content, while the CSTD group maintained the lowest MDA levels throughout storage. On day 10, the MDA contents were 14.39 nmol/g (Blank-S), 14 nmol/g (Blank-P), 11.53 nmol/g (CS-S), 11.23 nmol/g (CS-P), 9.43 nmol/g (CSTD-S), and 8.83 nmol/g (CSTD-P). This reduction in MDA levels under CSTD treatment reflects the film's ability to inhibit lipid peroxidation and oxidative stress, effectively protecting the cellular membrane. These results align with the findings of Fu et al. (Fu et al., 2023), where a multifunctional cinnamaldehyde-tannic acid chitosan composite film reduced MDA accumulation during mushroom storage, demonstrating the film's protective effect against oxidative damage.

The total phenolic content (TPC) trends are shown in Fig. 7(D). The initial TPC value was 120 mg GAE/g, with the Blank group showing an initial increase followed by a decline, peaking on day 4 at 214 mg GAE/g (Blank-S) and 224 mg GAE/g (Blank-P). The CS group exhibited a similar pattern, peaking on day 6 at 228 mg GAE/g (CS-S) and 237 mg GAE/g (CS-P). Notably, the CSTD group maintained an upward trend throughout the 10-day storage period, with final TPC values of 245 mg GAE/g (CSTD-S) and 237 mg GAE/g (CSTD-P), significantly higher than both the Blank and CS groups. This preservation of phenolic content highlights the antioxidant potential of the CSTD film, as it not only prevents phenolic compound degradation but also enhances the fruit's antioxidant defense mechanisms. Similar results were reported by Shiv et al. (Shankar, Khodaei, & Lacroix, 2021), where chitosan films incorporating essential oil and nano-silver effectively preserved phenolic compounds in strawberries.

Fig. 7(F) illustrates the variation in total flavonoid content (TFC). Initially, TFC was 0.4 mg RE/g, and its trend mirrored that of total phenolic content (TPC). The Blank and CS groups peaked on days 4 and 6, respectively, while the CSTD group exhibited a continuous increase throughout the 10-day period. On day 10, TFC values were 1.55 mg RE/g (Blank-S), 1.73 mg RE/g (Blank-P), 1.86 mg RE/g (CS-S), 2.02 mg RE/g (CS-P), 3.31 mg RE/g (CSTD-S), and 3.18 mg RE/g (CSTD-P). The CSTD film demonstrated a remarkable ability to preserve flavonoids, with levels more than double those of the Blank group. This outcome aligns with the findings of Xing et al. (Xing et al., 2020), where a chitosan/nano-TiO_2 composite film effectively enhanced TFC in mangoes, suggesting that the film's protective structure mitigated TFC degradation.

In summary, the CSTD film effectively protects against oxidative stress by inhibiting lipid peroxidation and preserving phenolic and flavonoid compounds. Its dense, UV-blocking structure reduces oxygen and UV exposure, slowing oxidative reactions. Additionally, the antioxidant properties of DEO and nano-TiO_2 enhance the fruit's internal antioxidant capacity, maintaining higher TPC and TFC levels, thus improving storage quality and extending the shelf life of *Actinidia arguta*. Similar preservation effects have been observed in other small berries, such as the study by Li et al.(Hanyu et al., 2024). on the preparation of chitosan-based Pickering emulsion coatings for strawberry preservation and the study by Xing et al.(Xing et al., 2021) on "Effect of Chitosan/Nano-TiO_2 Composite Coating on the Postharvest Quality of Blueberry Fruit," which showed that similar antioxidant mechanisms and UV-blocking properties are effective in extending shelf life. Based on these findings, it can be inferred that the CSTD film may also have preservation potential for other small berries, offering a promising solution for maintaining their quality during storage and transportation.

4. Conclusion

The study successfully developed and characterized chitosan-based nanocomposite films incorporating nano-TiO_2 and DEO for the preservation of soft date kiwi fruit. The improved structural, thermal, and physical properties of the composite film were confirmed by a combination of FT-IR, XRD, SEM, TGA, UV–visible, and WCA, and a cross-linking interaction between the CS with titanium dioxide nanoparticles and DEO occurred.

Notably, the addition of nano-TiO_2 and DEO significantly enhanced the films' mechanical strength, and antimicrobial, and antioxidant properties.

When used on soft date *Actinidia arguta*, the composite films

exhibited significant freshness preservation effects, including reduced weight loss, firmness retention, reduced spoilage, reduced total microbial counts, stabilized respiration rates, and better retention of TSS, VC, and TA, and the films effectively regulated enzyme activity. In summary, the shelf life of soft date *Actinidia arguta* was extended to 10 d and the storage quality of soft date *Actinidia arguta* was improved.

These findings suggest that CSTD offers a viable, natural, and eco-friendly solution for food preservation, potentially reducing food waste and enhancing the commercial value of perishable fruits. Future research should focus on optimizing the composite formulation.

CRediT authorship contribution statement

Yue Wang: Writing – original draft. **Yu Zhang:** Conceptualization. **Yaomei Ma:** Data curation. **Jiaxin Liu:** Project administration. **Ruinting Zhang:** Writing – review & editing. **Jun Zhao:** Funding acquisition.

Declaration of competing interest

The authors declare that they have no known competing financial interests or personal relationships that could have appeared to influence the work reported in this paper.

Data availability

The datasets are available from the corresponding author upon reasonable request.

Acknowledgments

This research was funded by the Jilin Province Science and Technology Development Project (20210203135SF) and Study Abroad Fund Project [2023] No. 43 (202308220123).

References

Cao, R., Yan, L., Xiao, S., Hou, B., Zhou, X., Wang, W., … Zhang, J. (2023). Effects of different low-temperature storage methods on the quality and processing characteristics of fresh beef. *Foods, 12*(4), 782. https://doi.org/10.3390/foods12040782

Chang, X., Hou, Y., Liu, Q., Hu, Z., Xie, Q., Shan, Y., … Ding, S. (2021). Physicochemical and antimicrobial properties of chitosan composite films incorporated with glycerol monolaurate and nano-TiO2. *Food Hydrocolloids, 119*, Article 106846.

Dong, Z., Li, R., & Gong, Y. (2021). Antibacterial and freshness-preserving mechanisms of chitosan-nano-TiO2-nano-ag composite materials. *Coatings, 11*(8), 914.

Fu, H., Huang, R., Li, J., Lin, Z., Wei, F., & Lin, B. (2023). Multifunctional cinnamaldehyde-tannic acid nano-emulsion/chitosan composite film for mushroom preservation. *Food Hydrocolloids, 145*, Article 109111.

Gohargani, M., Lashkari, H., & Shirazinejad, A. (2020). Study on biodegradable chitosan-whey protein-based film containing bionanocomposite TiO2 and Zataria multiflora essential oil. *Journal of Food Quality, 2020*(1), Article 8844167.

Hanyu, L., Liu, M., Han, S., Hua, S., Zhang, H., Wang, J., … Meng, D. (2024). Edible chitosan-based pickering emulsion coatings: Preparation, characteristics, and application in strawberry preservation. *International Journal of Biological Macromolecules, 264*, Article 130672. https://doi.org/10.1016/j.ijbiomac.2024.130672

Heras, M., Huang, C.-C., Chang, C.-W., & Lu, K.-H. (2024). Trends in chitosan-based films and coatings: A systematic review of the incorporated biopreservatives, biological properties, and nanotechnology applications in meat preservation. *Food Packaging and Shelf Life, 42*, Article 101259.

Jovanović, J., Ćirković, J., Radojković, A., Mutavdžić, D., Tanasijević, G., Joksimović, K., … Branković, Z. (2021). Chitosan and pectin-based films and coatings with active components for application in antimicrobial food packaging. *Progress in Organic Coatings, 158*, Article 106349.

Li Hua, Z., Li, Y., Chen, T., Alamri, A. S., Xu, Y., … Hu, J. (2024). Development of multifunctional chitosan-based composite film loaded with tea polyphenol nanoparticles for strawberry preservation. *International Journal of Biological Macromolecules, 275*(Pt 2), Article 133648. https://doi.org/10.1016/j.ijbiomac.2024.133648

Li Wang, Y., Ma, Y., Zheng, N., Liu, J., & Liu, T. (2024). Preparation and characterization of chitosan-based corn protein composites constructed with TG enzyme and their preservation performance on strawberries. *International Journal of Biological Macromolecules, 270*, Article 132190. https://doi.org/10.1016/j.ijbiomac.2024.132190

Li Zhou, Y., Wang, Z., Cai, R., Yue, T., & Cui, L. (2021). Preparation and characterization of chitosan–nano-ZnO composite films for preservation of cherry tomatoes. *Foods, 10*(12), 3135.

Liu Cai, Z., Sheng, L., Ma, M., Xu, Q., & Jin, Y. (2019). Structure-property of crosslinked chitosan/silica composite films modified by genipin and glutaraldehyde under alkaline conditions. *Carbohydrate Polymers, 215*, 348–357. https://doi.org/10.1016/j.carbpol.2019.04.001

Liu Wang, S., Liang, H., Zhou, J., Zong, M., Cao, Y., & Lou, W. (2024). A review of advancements in chitosan-essential oil composite films: Better and sustainable food preservation with biodegradable packaging. *International Journal of Biological Macromolecules, 274*(Pt 2), Article 133242. https://doi.org/10.1016/j.ijbiomac.2024.133242

Liu, Z., Du, M., Liu, H., Zhang, K., Xu, X., Liu, K., … Liu, Q. (2021). Chitosan films incorporating litchi peel extract and titanium dioxide nanoparticles and their application as coatings on watercored apples. *Progress in Organic Coatings, 151*, Article 106103.

Macedo, C., Costa, P. C., & Rodrigues, F. (2023). Bioactive compounds from Actinidia arguta fruit as a new strategy to fight glioblastoma. *Food Research International, 175*, 113770.

Marinova, G., & Batchvarov, V. (2011). Evaluation of the methods for determination of the free radical scavenging activity by DPPH. *Bulgarian Journal of Agricultural Science, 17*(1), 11–24.

Mittal, A., Singh, A., Benjakul, S., Prodpran, T., Nilsuwan, K., Huda, N., & de la Caba, K. (2021). Composite films based on chitosan and epigallocatechin gallate grafted chitosan: Characterization, antioxidant and antimicrobial activities. *Food Hydrocolloids, 111*, Article 106384.

Park, D. H., Lee, S., Lee, J., Kim, E. J., Jo, Y.-J., Kim, H., … Hong, G.-P. (2021). Stepwise cooling mediated feasible supercooling preservation to extend freshness of mackerel fillets. *LWT, 152*, Article 112389.

Petriccione, M., De Sanctis, F., Pasquariello, M. S., Mastrobuoni, F., Rega, P., Scortichini, M., & Mencarelli, F. (2015). The effect of chitosan coating on the quality and nutraceutical traits of sweet cherry during postharvest life. *Food and Bioprocess Technology, 8*, 394–408.

Pinto, D., Delerue-Matos, C., & Rodrigues, F. (2020). Bioactivity, phytochemical profile and pro-healthy properties of Actinidia arguta: A review. *Food Research International, 136*, Article 109449. https://doi.org/10.1016/j.foodres.2020.109449

Roy, S., Zhai, L., Kim, H. C., Pham, D. H., Alrobei, H., & Kim, J. (2021). Tannic-acid-cross-linked and TiO2-nanoparticle-reinforced chitosan-based nanocomposite film. *Polymers, 13*(2), 228.

Sami, R., Elhakem, A., Alharbi, M., Benajiba, N., Fikry, M., & Helal, M. (2021). The combined effect of coating treatments to nisin, nano-silica, and chitosan on oxidation processes of stored button mushrooms at 4 C. *Scientific Reports, 11*(1), 1–9.

Shankar, S., Khodaei, D., & Lacroix, M. (2021). Effect of chitosan/essential oils/silver nanoparticles composite films packaging and gamma irradiation on shelf life of strawberries. *Food Hydrocolloids, 117*, Article 106750.

Sharma, R., & Dhamodharan, R. (2024). Tannic acid crosslinked chitosan-guar gum composite films for packaging application. *International Journal of Biological Macromolecules, 260*(Pt 1), Article 129317. https://doi.org/10.1016/j.ijbiomac.2024.129317

Soltani, Z., Tavakolipour, H., & Tabari, M. (2023). The influence of chitosan and titanium dioxide nanoparticles incorporated with polylactic acid on prolonging rye bread shelf life. *Journal of Food Measurement and Characterization, 17*(2), 1806–1816.

Song, H., Yuan, W., Jin, P., Wang, W., Wang, X., Yang, L., & Zhang, Y. (2016). Effects of chitosan/nano-silica on postharvest quality and antioxidant capacity of loquat fruit during cold storage. *Postharvest Biology and Technology, 119*, 41–48.

Sun, J., Li, Y., Cao, X., Yao, F., Shi, L., & Liu, Y. (2022). A film of chitosan blended with ginseng residue polysaccharides as an antioxidant packaging for prolonging the shelf life of fresh-cut melon. *Coatings, 12*(4), 468.

Thomas, R., Prabha, V. C., Sanuja, S., & Umapathy, M. (2023). Formation and characterization of novel antimicrobial chitosan/Moringa oleifera gum/nano silicon dioxide nanocomposite film for active food packaging. *Journal of Materials Research, 38*(13), 3372–3382.

Tian, F., Chen, W., Cai'E, W., Kou, X., Fan, G., Li, T., & Wu, Z. (2019). Preservation of Ginkgo biloba seeds by coating with chitosan/nano-TiO2 and chitosan/nano-SiO2 films. *International Journal of Biological Macromolecules, 126*, 917–925.

Wang, Y., Tang, J., Zeng, Y., Liu, X., Chen, M., Dai, J., … Liu, Y. (2023). Nanofibrous composite membranes based on chitosan-nano zinc oxide and curcumin for Kyoho grapes preservation. *International Journal of Biological Macromolecules, 242*(Pt 2), Article 124661. https://doi.org/10.1016/j.ijbiomac.2023.124661

Wang, Y., Wang, J., Lai, J., Zhang, X., Wang, Y., & Zhu, Y. (2022). Preparation and characterization of chitosan/whey isolate protein active film containing TiO(2) and white pepper essential oil. *Frontiers in Nutrition, 9*, Article 1047988. https://doi.org/10.3389/fnut.2022.1047988

Wang Yang, Z., Zhang, C., Zhai, X., Zhang, X., Huang, X., … Shi, J. (2022). Chitosan-cinnamon essential oil/sodium alginate-TiO2 bilayer films with enhanced bioactive retention property: Application for mango preservation. *International Journal of Biological Macromolecules, 222*, 2843–2854.

Wang Yuan, Y., Liu, Y., Li, X., & Wu, S. (2024). Application of chitosan in fruit preservation: A review. *Food Chem X, 23*, Article 101589. https://doi.org/10.1016/j.fochx.2024.101589

Xing, Y., Yang, H., Guo, X., Bi, X., Liu, X., Xu, Q., … Shui, Y. (2020). Effect of chitosan/Nano-TiO2 composite coatings on the postharvest quality and physicochemical characteristics of mango fruits. *Scientia Horticulturae, 263*, Article 109135.

Xing, Y., Yang, S., Xu, Q., Xu, L., Zhu, D., Li, X., … Bi, X. (2021). Effect of chitosan/nano-TiO2 composite coating on the postharvest quality of blueberry fruit. *Coatings, 11*(5), 512. https://doi.org/10.3390/coatings11050512

Xing, Y., Yue, T., Wu, Y., Xu, Q., Guo, X., Wang, X., … Yang, P. (2021). Effect of chitosan composite coatings with salicylic acid and titanium dioxide nanoparticles on the storage quality of blackcurrant berries. *Coatings, 11*(6), 738.

Xiong, S., Zhou, F., Jiang, A., Yang, L., & Hu, W. (2024). Ethanol vapor ameliorates chilling injury and maintains postharvest quality by increasing antioxidant capacity of hardy kiwifruit (Actinidia arguta). *Scientia Horticulturae, 327*, Article 112796.

Xue, Y., Wu, Z., Feng, & Kou. (2023). The characterization of antimicrobial nanocomposites based on chitosan, cinnamon essential oil, and TiO(2) for fruits preservation. *Food Chemistry, 413*, Article 135446. https://doi.org/10.1016/j.foodchem.2023.135446

Youssef, A. M., El-Sayed, H. S., El-Sayed, S. M., Fouly, M., & El-Aziz, M. A. (2023). Novel bionanocomposites based on cinnamon nanoemulsion and TiO2-NPs for preserving fresh chicken breast fillets. *Food and Bioprocess Technology, 16*(2), 356–367.

Zhang, L., Liu, Z., Wang, X., Dong, S., Sun, Y., & Zhao, Z. (2019). The properties of chitosan/zein blend film and effect of film on quality of mushroom (Agaricus bisporus). *Postharvest Biology and Technology, 155*, 47–56.

Zhao, J., Wang, Y., Li, J., Lei, H., Zhen, X., Gou, D., & Liu, T. (2023). Preparation of chitosan/Enoki mushroom foot polysaccharide composite cling film and its application in blueberry preservation. *International Journal of Biological Macromolecules, 246*, Article 125567.

Zhao Wang, Y., Li, J., Lei, H., Zhen, X., Gou, D., & Liu, T. (2023). Preparation of chitosan/Enoki mushroom foot polysaccharide composite cling film and its application in blueberry preservation. *International Journal of Biological Macromolecules, 246*, Article 125567. https://doi.org/10.1016/j.ijbiomac.2023.125567

Zhou, S.-D., Xu, X., Lin, Y.-F., Xia, H.-Y., Huang, L., & Dong, M.-S. (2019). On-line screening and identification of free radical scavenging compounds in Angelica dahurica fermented with Eurotium cristatum using an HPLC-PDA-triple-TOF-MS/MS-ABTS system. *Food Chemistry, 272*, 670–678.